# State of Florida hurricane loss projection model: Atmospheric science component

Mark Powell[a],*, George Soukup[a], Steve Cocke[b],
Sneh Gulati[c], Nirva Morisseau-Leroy[d], Shahid Hamid[c],
Neal Dorst[a], Lizabeth Axe[b]

[a]NOAA Hurricane Research Division, Miami, FL, USA
[b]Florida State University, Tallahassee, FL, USA
[c]Florida International University, Miami, FL, USA
[d]University of Miami, Miami, FL, USA

## Abstract

The State of Florida has developed an open, public model for the purpose of probabilistic assessment of risk to insured residential property associated with wind damage from hurricanes. The model comprises atmospheric science, engineering, and financial/actuarial components and is planned for submission to the Florida Commission on Hurricane Loss Projection Methodology. The atmospheric component includes modeling the track and intensity life cycle of each simulated hurricane within the Florida threat area. When a model storm approaches within a damage threshold distance of a Florida zip code location, the wind field is computed by a slab model of the hurricane boundary layer coupled with a surface layer model based on the results of recent GPS sonde research. A time series of open terrain surface winds is then computed for each zip code in the threatened area. Depending on wind direction, an effective roughness length is assigned to each zip code based on the upstream fetch roughness as determined from remotely sensed land cover/land use products. Based on historical hurricane statistics, thousands of storms are simulated allowing determination of the wind risk for all residential zip code locations in Florida. The wind risk information is then

*Corresponding author. Tel.: +1 305 361 4403; fax: +1 305 361 4402.

*E-mail address:* mark.powell@noaa.gov (M. Powell).

provided to the engineering and loss models to assess damage and average annual loss, respectively.
Published by Elsevier Ltd.

## 1. Introduction

The historical record for establishing the risk of hurricanes throughout the coastal United States is limited to a period of about 100 years, with relatively reliable and complete records [1]. Unfortunately, this period is not sufficient to establish risk without large errors so alternative methods have been used since the 1970s [2,3]. Hurricane risk models are currently used to conduct simulations of thousands of years of storms based on probability distributions of important historically observed parameters. This method is often referred to as the joint probability method since the probability of having an event is coupled with the probability that the event is of a given intensity. Commercial modeling interests have developed several versions of these which are used to advise the insurance industry for ratemaking. Unfortunately, the models are proprietary so customers whose rates have increased on the basis of model calculations have no way of examining or questioning the results. The State of Florida is developing a public model to provide an understandable baseline for comparison to the commercial models. The model will be open and transparent, in which methods and results can be examined in great detail. The Hurricane Loss Projection Model consists (Fig. 1) of independent modules for atmospheric science, engineering, and actuarial components. Each component provides one-way input to the next component in line until the end result (average annual loss per zip code) is achieved. This paper will describe the atmospheric science component of the model.

## 2. Threat area

To focus on storms capable of causing residential property damage in Florida, a threat area is defined to best capture the statistical characteristics of historical tropical cyclones that have affected the state. The area within 1000 km of a location (26.0 N, 82.0 W) off the southwest coast of Florida (Fig. 2) was chosen since this captures storms that can affect the panhandle, west, and northeast coasts of Florida, as well as storms that approach South Florida from the vicinity of Cuba and the Bahamas. A model flow chart (Fig. 3) describes the order of calculations for the atmospheric science component.

## 3. Annual occurrence

The model has the capability of simulating climate cycles and tropical cyclone activity according to different periods of the historical record [4]. The historical record

**State of Florida Hurricane Loss Projection Model**

**Atmospheric Science Component I**
Storm genesis
Movement
Intensity

**Atmospheric Science Component II**
Wind Field
Zip Code time series
Terrain influences
Probabilities of exceedence

**Engineering Component**
Inventory of residential construction
Damage when wind load exceeds
resistance

**Financial/Actuarial Component**
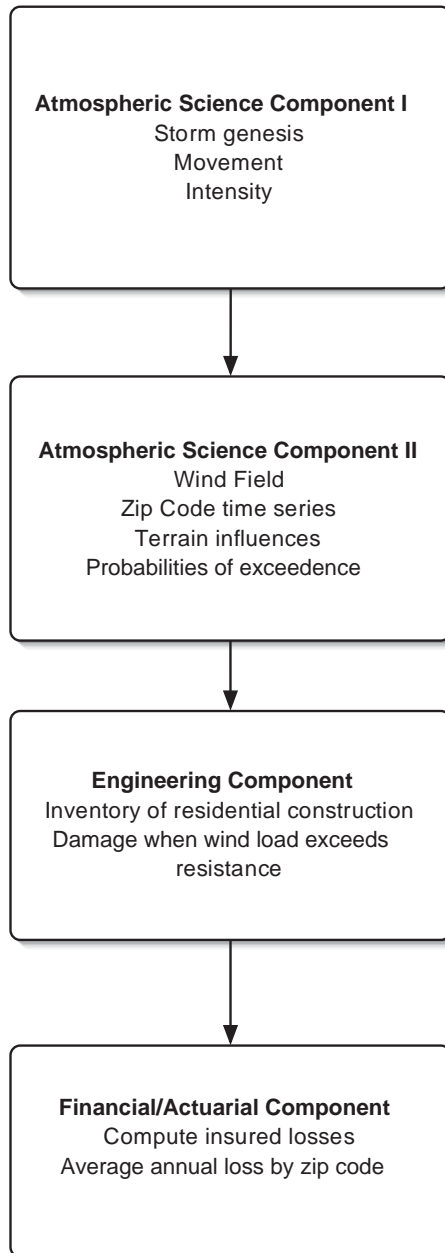Compute insured losses
Average annual loss by zip code

Fig. 1. Flow chart depiction of independent modules of the State of Florida Hurricane Loss Projection Model.
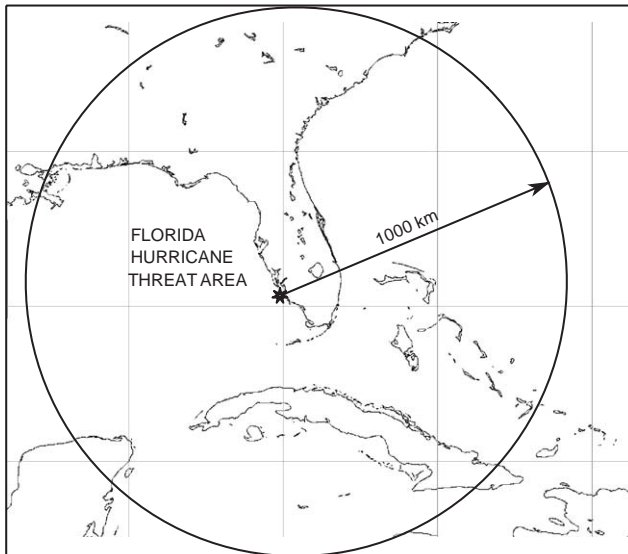
Fig. 2. Threat area map. All storms entering or developing within the threat area are considered for characteristics relating to formation, movement, and intensity.

for the Atlantic tropical cyclone basin (known as "HURDAT") is a six hourly record of tropical storm and hurricane positions and intensities [5], which are expressed as estimated maximum 1 min surface (10 m) winds and, when available, central sea level pressure. The period 1851–2004 is the largest available, but the period 1900–2004 is most often used due to uncertainties about 19th century storms, especially for Florida, due to a lack of population centers and meteorological measurements of hurricanes before the start of the 20th century. There are also uncertainties about the first half of the 20th century since aircraft reconnaissance only began in the 1940s so another choice in the period of record are the years 1944–2004. Four additional choices are available which simulate the warm (El Nino, fewer hurricanes) and neutral or cold (La Nina, more hurricanes) inter annual climate cycles in tropical cyclone activity, as well as the cold or warm phases of the Multi-decadal climate cycles. These choices are primarily for research purposes and constrain the historical record to use only years with the specified climate cycle to fit annual tropical cyclone occurrence. For insurance applications the 1900-prior year period will be of most interest (e.g. for the 2005 season, the period 1900–2004 would be of interest if the 2004 season official hurricane tracks are available). Two fits are tested to the annual hurricane occurrence frequency distribution: the negative binomial and the Poisson model. Chi-square goodness of fit tests determine which fit is used for the subsequent simulations. The chosen fit is then randomly sampled to determine how many storms occur for each year of the simulation. Once the number of tropical cyclones within the threat area for a given year is determined, the date and time of genesis is computed from an empirical distribution based on historical storm tracks.
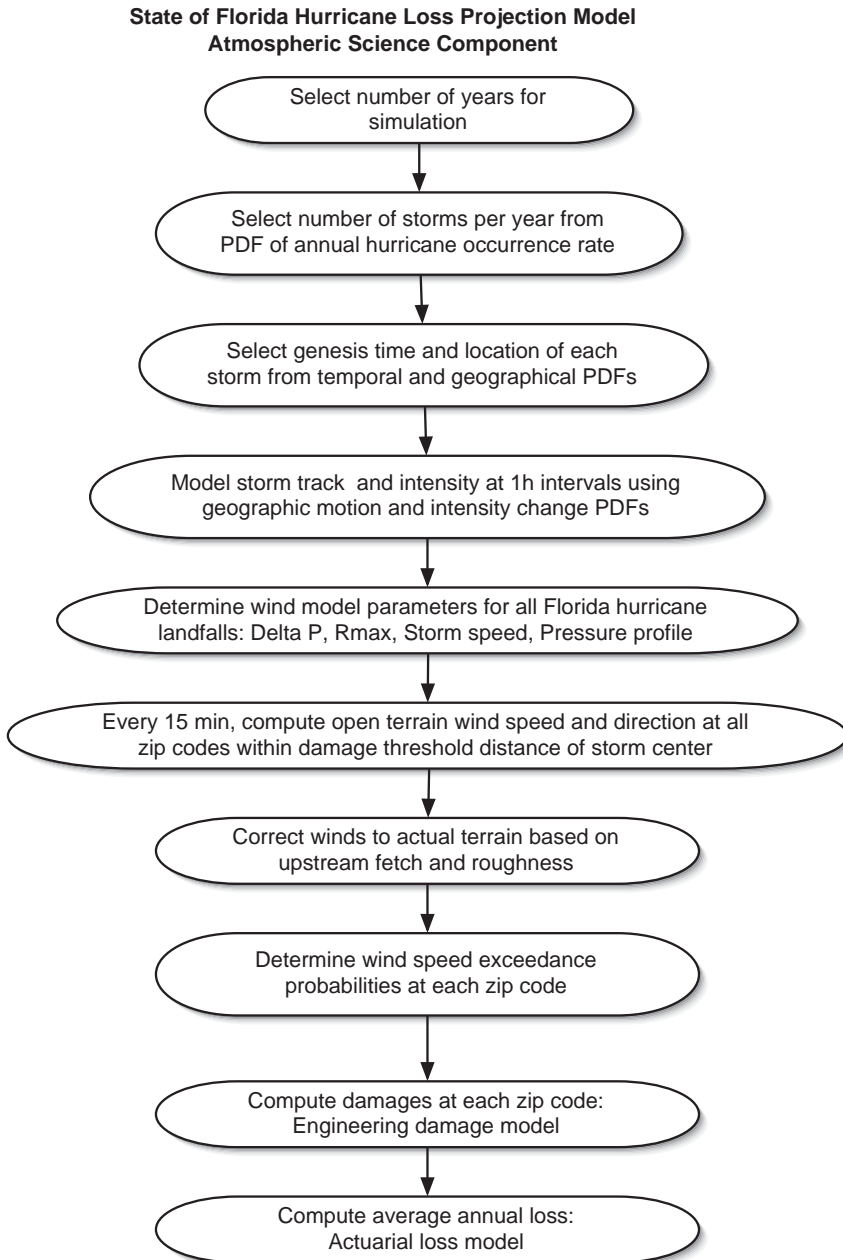
**State of Florida Hurricane Loss Projection Model**
**Atmospheric Science Component**

Select number of years for simulation

Select number of storms per year from PDF of annual hurricane occurrence rate

Select genesis time and location of each storm from temporal and geographical PDFs

Model storm track and intensity at 1h intervals using geographic motion and intensity change PDFs

Determine wind model parameters for all Florida hurricane landfalls: Delta P, Rmax, Storm speed, Pressure profile

Every 15 min, compute open terrain wind speed and direction at all zip codes within damage threshold distance of storm center

Correct winds to actual terrain based on upstream fetch and roughness

Determine wind speed exceedance probabilities at each zip code

Compute damages at each zip code: Engineering damage model

Compute average annual loss: Actuarial loss model

Fig. 3. Flow chart depiction of the atmospheric science component of the State of Florida Hurricane Loss Projection Model.

## 4. Storm genesis, movement, and intensity

The threat area is divided into regions that contain the historical and seasonal characteristics of storm motion and intensity change. Initial location, intensity, and motion for each storm are based on the geographic probability distributions of each quantity for a given time within the season. Intensity is initially modeled as the gradient of pressure $\Delta p$, the difference between the central minimum sea level pressure and an outer peripheral pressure (assumed to be 1013 hPa). Ultimately (after the wind model is run) the intensity is defined according to the maximum surface wind speed in the storm. Hurricane tracks are modeled as a Markov process. We use a stochastic approach to model the storm genesis location and track and central pressure evolution. A probability distribution function (PDF) for the initial storm position is derived from the historical ''genesis'' data. Here, we define genesis as the time when a hurricane forms in or first appears in the threat area. The PDF is derived for $0.5°$ latitude/longitude box regions, as well as time of season (month). A (uniform) random error term is added so that the storm may form anywhere within the $0.5°$ box. Fig. 4 shows a plot of the spatial PDF for storm genesis locations in the threat area for the month of August.

We derive discrete PDFs based on historical data to provide the initial and subsequent motion and intensity of the storm. A storm is simulated by repeatedly sampling from these PDFs via a Monte Carlo approach. These PDFs are derived for variable-sized regions centered at every $0.5°$ latitude and longitude in the hurricane basin. The size of these regions is determined to be that which gives a robust probability density function (PDF) for the quantities of interest (speed, direction, and central pressure), up to some maximum size. Once the storm has been given an initial condition, its subsequent evolution is governed by sampling the PDFs for changes in intensity, translation speed, and heading angle in 1-h increments.

Intensity change is modeled by using the observed geographic probability distribution of 6-h changes of central pressure as related to the relative intensity, a measure of how close the storm comes to meeting its maximum possible intensity (potential intensity) [6]. Potential intensity takes into account the concept of the hurricane as a heat engine constrained by the input (sea surface) and outflow (upper troposphere) temperatures. Intensity change is limited so as to not exceed the maximum observed change for a particular geographic region. When a storm center crosses the coastline (landfall) the intensity change follows a pressure decay model (discussed below). If the storm moves back over the sea, the former intensity change model is reinstated. A storm need not make landfall to be considered however; bypassing hurricanes are considered that never make landfall, or make landfall well before or well after producing damaging winds at a particular zip code.

The PDFs for change in storm translation speed and direction depend on the current speed and direction (binned in discrete intervals), as well as geographic location ($0.5°$ lat-lon location) and time of season (month). Fig. 5 shows a PDF for change in direction for eight possible direction intervals ($45°$ intervals). The PDF
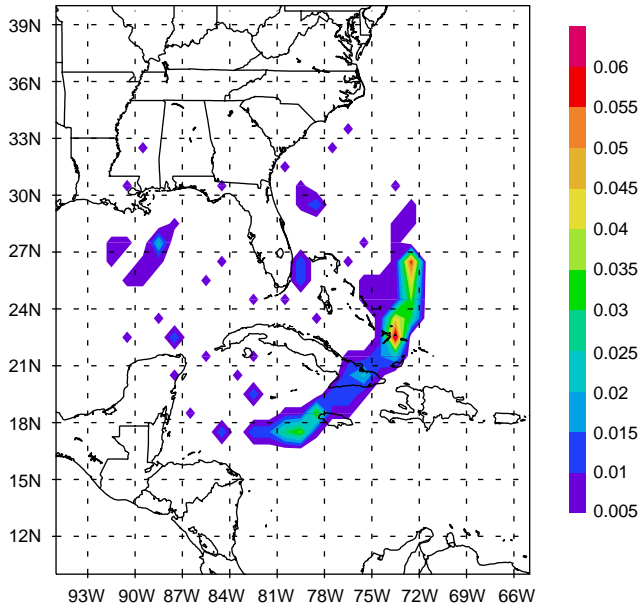
Fig. 4. Geographic distribution of probability of a storm entering or developing within the threat area during the month of August based on the historical period 1900–2000.
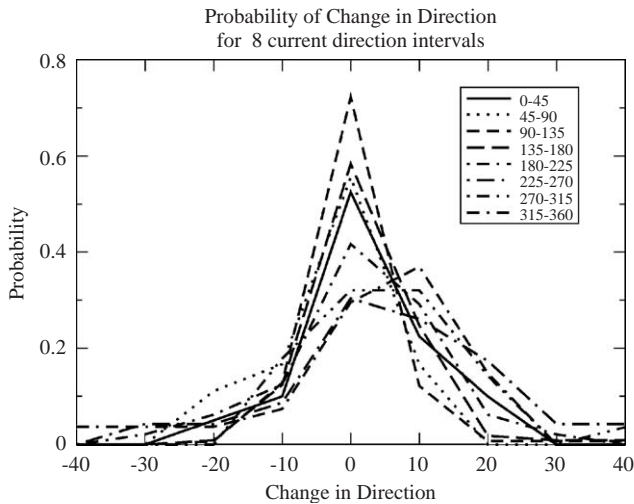


Fig. 5. Probability of a change in direction of storm motion (over a 6 h time period) to the left or right of the current motion as a function of the current storm heading (in degrees from north).

indicates that the storm has a high probability for maintaining current direction, except for westward traveling storms which tend to turn right (northward) somewhat.

Our approach has a great advantage over early models [2,3] that considered a circular approach region surrounding coastal cities. Storms that parallel the coast or make several landfalls can be properly simulated with our method.

## 5. Storm decay

The tropical ocean is typically warmer than the air above it, enabling a transfer of heat and moisture to the air. Inflow towards the center of the tropical cyclone transports this energy toward the eyewall, where it can help sustain convection, leading to a positive feedback of warming in the eye, lower minimum central pressure, stronger inflow, and more energy transport [7,8]. Over the ocean this positive feedback loop may be slowed or reversed by ocean cooling, advection of relatively cold dry air with a history of travel over land, or strong wind shear that prevents the storm center from focusing heating in the eye [9,10]. As a hurricane makes landfall, the circulation traverses land, and the storm loses its source of energy [11]. More and more dry and relatively cool air flows towards the center, causing the air to cool as it expands adiabatically while approaching lower pressures [12]. The result is that the eye heating gradually decreases and the central pressure begins to increase or "fill".

Since the wind model depends on the specification of the pressure gradient, a method was needed to estimate the central pressure over land. As a starting point for a simple decay model we will use the exponential decay as a function of time after landfall developed by Vickery and Twisdale [13]. The HURDAT database and Ho et al. [14] contains documentation of storm decay and pressure filling for many hurricane landfall cases in the historical record. Vickery and Twisdale [13] developed and tested a model for the Florida peninsula based on nine landfalling hurricanes and found the model to be slightly conservative (larger values) within 3 h of landfall and slightly non-conservative (smaller values) beyond 3 h after landfall. The form of the model is

$$\Delta p(t) = \Delta p_0 \exp(-at), \tag{1}$$

where $\Delta p(t)$ is the time-dependent central pressure deficit and $t$ represents the time after landfall. The filling rate constant is given as

$$a = a_0 + a_1 \Delta p_0 + \varepsilon, \tag{2}$$

where $\varepsilon$ is a random error term with a normal distribution. The dependence of the filling rate constant on $\Delta p_0$ allows stronger storms to decay faster than weak storms; a characteristic observed in hurricane landfalls [15]. The random error term allows for the possibility that some storms will decay slower or faster than average. For the Florida peninsula Vickery and Twisdale [13] use $a_0 = 0.006$, $a_1 = 0.00046$, and the standard deviation of 0.0025.

The Kaplan and DeMaria [16] model is also pertinent but it deals with wind decay rather than pressure decay and there is no well-established method to convert inland-decayed peak winds to central pressure. The advantage of the filling model is that it

provides a starting point to invoke an intensity redevelopment for storms that exit the coastline and re-intensify over water. When a storm reemerges over water, the intensity is modeled along the track the same way it was before landfall using the decayed pressure as an initial value.

## 6. Damage distance threshold

To save computing resources, the wind field is not evaluated unless a hurricane passes within a distance from the storm at which damage might be possible, the damage distance threshold. Hurricanes come in a variety of sizes and shapes, so a fixed distance criterion may not be practical, since it may be unnecessarily large for small storms. As an alternative, we describe the damage distance threshold ($D$) as a function of the radius of maximum wind speed ($R_{max}$). For small storms with small $R_{max}$ we will go outward from the storm center $\sim 10\ R_{max}$ and for large storms we will go out a as far as $4\ R_{max}$.

Twelve hurricanes comprising a variety of storm structures and shapes were evaluated by comparing HRD Hurricane Wind Analysis System (H*Wind) analyses of the outermost radius of marine exposure 25 m/s sustained winds. For hurricanes with $R_{max} > 50$ km, $D$ is held constant at $4\ R_{max}$. For $R_{max} < 48$ km,

$$D = 12.323 - 0.162 R_{max}. \tag{3}$$

The 25 m/s sustained marine wind speed contour represents a 1 h mean marine wind of 21 m/s. This wind speed is assumed to represent the mean marine exposure wind speed at which light damage begins. The equivalent 1 h mean wind for roughness representative of Florida zip codes is $\sim 14.5$ m/s.

## 7. Wind field model

The model is based on the slab boundary layer concept originally conceived by Ooyama [17] and implemented by Shapiro [18]. Similar models based on this concept have been developed by Thompson and Cardone [19] and Vickery et al. [20,21]. As in Ref. [18], the model is initialized by a boundary layer vortex in gradient balance. Gradient balance represents a circular flow caused by the balance of forces whereby the inward directed pressure gradient force is balanced by outward Coriolis and centripetal accelerations. The coordinate system translates with the hurricane vortex moving at velocity $\vec{c}$. The vortex translation is assumed to equal the geostrophic flow associated with the large-scale pressure gradient. As a possible future enhancement the large-scale flow in which the vortex is embedded may be treated independently of the vortex motion as in Ref. [19]. In cylindrical coordinates that translate with the moving vortex, equations for a slab hurricane boundary layer under a prescribed pressure

gradient [18] are

$$\frac{u\partial u}{\partial r} - \frac{v^2}{r} - fv + \frac{v}{r}\frac{\partial u}{\partial \phi} + \frac{\partial p}{\partial r} - K\left(\nabla^2 u - \frac{u}{r^2} - \frac{2}{r^2}\frac{\partial u}{\partial \phi}\right) + F(\vec{c}, u) = 0 = \frac{\partial u}{\partial t}, \qquad (4)$$

$$u\left(\frac{\partial v}{\partial r} + \frac{v}{r}\right) + fu + \frac{v}{r}\frac{\partial v}{\partial \phi} - K\left(\nabla^2 v - \frac{v}{r^2} + \frac{2}{r^2}\frac{\partial u}{\partial \phi}\right) + F(\vec{c}, v) = 0 = \frac{\partial v}{\partial t}, \qquad (5)$$

where $u$ and $v$ are the respective radial and tangential wind components relative to the moving storm, $p$ is the sea-level pressure which varies with radius ($r$), $f$ is the Coriolis parameter which varies with latitude, $\phi$ is the azimuthal coordinate, $K$ is the eddy diffusion coefficient, and $F(c,u)$, $F(c,v)$ are frictional drag terms (discussed below). All terms are assumed to be representative of means through the boundary layer. The motion of the vortex is determined by the modeled storm track.

Note that Eqs. (4) and (5) represent a steady-state solution. In order to solve the equations, they must be integrated until the steady state assumption is satisfied either through time integration (e.g., see Refs. [18,19]) or numerical method (see Appendix A). More sophisticated multiple level models (e.g., see Ref. [22]) include equations describing the thermodynamic processes including convection, cloud and precipitation microphysics, evaporation of sea spray, exchange of heat and moisture with the sea, etc. These processes interact to change the pressure and wind fields over time, but the computational requirements of such models make them poorly suited for risk assessment. An advantage of our approach is that the solution to (4) and (5) is straightforward and we do not have the computationally costly requirement to run the model to "steady state" each time we desire a solution. A limitation of our model (and all other Hurricane risk models) is the lack of physical representation of additional processes that may influence the wind field of a tropical cyclone.

## 7.1. Surface pressure field

The symmetric pressure field $p(r)$ is specified as

$$p(r) = p_0 + \Delta p e^{(R_{max}/r)^B} \qquad (6)$$

where $p_0$ is the central minimum sea level pressure, $B$ is the Holland [23] pressure profile shape parameter, $R$ is the radius of maximum wind speed (in nautical miles), and $\Delta p$ is the pressure deficit defined earlier. The central pressure is modeled according to the intensity modeling in concert with the storm track.

The mean tangential gradient wind is determined primarily by (6). A recent publication by Willoughby and Rahn [24] of the NOAA-HRD database of research and reconnaissance aircraft measurements was supplemented with central pressure measurements and $R_{max}$ values adjusted for tilt between the surface and the 3 km level. These data were then cut to be more relevant to our model. We retained 201 profiles with maximum winds $> 33$ m/s, with flight levels below the 700 hPa pressure surface, and with Atlantic basin latitudes 15–35 N and longitudes west of 60° West. The resulting expression for $B$ explains 20% of the variance:

$$B = 1.881093 - 0.010917\,\text{Lat} - 0.005567\,R_{max} + \varepsilon, \qquad (7)$$

where Lat is the latitude and ε is a random term from a zero mean normal distribution with a standard deviation of 0.286. $B$ is censored to remain above 0.8 and below 2.2.

## 7.2. Radius of maximum wind

The radius of maximum wind is determined from a distribution of landfall values as a function of $p_0$ and latitude. As in Ref. [21], a log normal distribution is assumed for $R_{max}$ with a mean value determined as a function of $p$ and latitude. In developing the models for $R_{max}$, we used the data from Ref. [14] for storms from 1900 to 1983; NOAA-HRD archives of realtime surface wind analyses from 1995 to 2002; an "extended best track" archive of the National Hurricane Center that was maintained by Dr. Mark DeMaria [25] (now with NOAAs NESDIS at Colorado State University) for the years 1988–1999; and an HRD archive of aircraft observations for the years 1984–1987. To create a model to describe $R_{max}$ we considered Gulf of Mexico and US Atlantic coast hurricane landfalls with latitudes as high as 34° North in order to help fill a dearth of information on storms affecting the Northeast Florida coastline. The relationship between $R_{max}$ and $p$ and latitude shows much scatter but a generalized linear model for the natural log of $R_{max}$ ($r^2 = 0.212$) provides a useful estimation:

$$\ln R_{max} = 2.0633 + 0.0182\Delta p - 0.00019008\Delta p^2 + 0.0007336\text{Lat}^2 + \varepsilon, \quad (8)$$

where ε is a normal random variable with a mean of zero and a standard deviation of 0.3. Eq. (7) describes the mean of the log normal distribution of $R_{max}$ in nautical miles. When a simulated storm is close enough to land to become a threat, an $R_{max}$ value is randomly chosen given the $p$ and latitude. $R_{max}$ is computed at each time step but the random error term is computed only once for each landfall. $R_{max}$ is censored to remain below 102 km and above 7.4 km.

## 7.3. Friction terms

The frictional drag is in the direction opposite the total wind relative to the earth at the surface and represents the mean momentum flux from the atmosphere to the surface. The frictional terms in (3) and (4) may be specified in terms of the vertical gradient of stress:

$$F(\vec{c}, u) = \frac{\partial \tau}{\partial z}. \quad (9)$$

The variation of τ with height over the depth of the slab boundary layer may be described by a function with properties supported by observations in the surface layer of tropical cyclones. The lower 250 m of the boundary layer is occupied by a surface layer in which stress is approximately constant. In reality, the stress is greatest close to the surface, and is zero at the top of the boundary layer. By assuming stress as near constant over the surface layer we satisfy conditions for applying the logarithmic wind profile to describe the vertical variation of the mean

wind speed with height. The fact that a mean logarithmic wind profile has been observed in tropical cyclone eyewalls [26] provides justification for the surface layer concept. The evaluation of (9) is approximated as 0.25 ($\tau_{\mathrm{sfc}}/h$), where $\tau_{\mathrm{sfc}}$ is the surface stress and $h$ represents the top of the boundary layer. Based on the mean height of the wind maximum in the hurricane eyewall in [26], an $h$ value of 500 m is justified. The factor 0.25 is based on judgment and takes into account the fact that the average stress in the slab boundary layer is less than the mean stress of the surface layer. This factor is consistent with preliminary calculations of the stress profile in the boundary layer derived from GPS sonde observations described in [26]. Other modelers using the slab boundary layer approach have used 0.3 [13] and 1.0 [18]. At the surface, the stress may be expressed in terms of the earth-relative surface wind velocity $U_{10}$ at a height of 10 m above the surface, and the neutral stability surface drag coefficient, $C_{\mathrm{d}}$:

$$\tau_{\mathrm{sfc}} = \rho C_{\mathrm{d}} \left| \vec{U}_{10} + \vec{c} \right| \left( \vec{U}_{10} + \vec{c} \right), \tag{10}$$

$$F(c, u) = \frac{\partial \tau}{\partial z} = 0.25 \frac{\tau}{h}, \tag{11}$$

where $C_d$ is specified by Large and Pond [27] and $U_{10}$ is the neutral stability surface (10 m, 32 ft) wind speed relative to the moving storm.

## 7.4. Eddy diffusion

The wind model describes the effects of horizontal turbulence following Shapiro [18]. In theory the role of eddy diffusion is to represent horizontal turbulent mixing in the radial and tangential directions. Vertical turbulent mixing (contained in the friction terms discussed earlier) is typically much larger in magnitude and is associated with a large body of research based on numerous field investigations. Horizontal mixing is most prominent in regions with strong horizontal gradients. Hence, the greatest impact of eddy mixing will be in the eyewall where radial gradients are strong. In practice, this term primarily serves as a way to smooth out computational noise in the model results but future enhancements might include a dependence on horizontal shear or grid spacing.

## 7.5. Model implementation

The hurricane wind field model is based on a fully two dimensional, time-independent, scaled version of the tangential and radial momentum equations (4) and (5) for the mean boundary layer wind components (see Appendix A for a complete description). The model makes use of a polar coordinate representation grid centered on the moving cyclone. The nested circles are separated from their inscribed and circumscribed neighbors by a radial separation of 0.1 $R/R_{\max}$; the azimuthal interval of the radial spokes is $10°$.
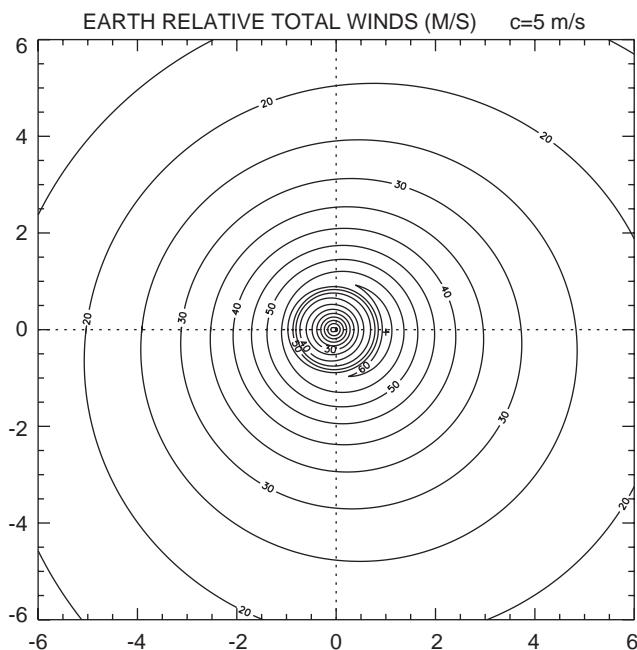
EARTH RELATIVE TOTAL WINDS (M/S)        c=5 m/s

Fig. 6. Horizontal distribution of mean surface wind speed, relative to a storm moving northward at 5 m/s. Horizontal coordinates are scaled by the radius of maximum wind.

Implementation proceeds according to the following steps: First, based on the input parameters, $R_{max}$, $p_0$, and $B$, radial profiles of the radial and tangential winds are calculated based on a stationary cyclone over open water to provide an "envelope" with which to set the size of the cyclone vortex. The wind field produced by these profiles is radially symmetric.

Azimuthal variation is introduced through the use of two form factors. The form factors multiply the radial and tangential profiles described above and provide a "factorized" ansatz for both the radial and tangential storm-relative wind components. Each form factor contains three constant coefficients which are variationally determined in such a way that the ansatz constructed satisfies (as far as its numerical degrees of freedom permit) the scaled momentum equations for the storm-relative polar wind components. The azimuthal variable ($\phi$) has its usual mathematical meaning such that increases from left to right with the rectangular X-axis aligned ( = 180, 0) and the Y-axis aligned ( = 270, 90) with Y increasing in the direction of storm translation.

The storm translation vector is added to the storm-relative wind components in order to obtain the earth-relative wind field. The translational motion of the storm is incorporated in the surface friction terms in the momentum equations which depend on the and are specific for the direction of storm translation which is aligned with the Y-axis. The wind field grid is then rotated so that the computational Y-axis coincides with the actual direction of motion of the cyclone center. The wind field thus far

constructed (Fig. 6) usually shows the location of peak winds to be to the right or forward edge of the right-rear quadrant of the cyclone.

### 7.6. Asymmetries in the wind field

The solution of (4) and (5) exhibits a shift of the radius of maximum winds toward the center when compared with the gradient wind profile. The tangential winds are also super gradient due to the advection inward of angular momentum induced by the frictional convergence. Besides vortex translation, radial advection of tangential momentum, and differential friction, other factors affecting the asymmetric distribution of winds in a tropical cyclone include synoptic scale vertical shear of the horizontal wind, synoptic scale weather features (e.g. a strong high pressure ridge to one side of the hurricane), rain band convection, concentric eyewall cycles, mesoscale variations in air-sea temperature difference, and tertiary circulations associated organized linear flow features and turbulent eddies. In the simple model described here, only the motion and differential friction influences are taken into account. The remaining features are difficult to parameterize and may be computationally prohibitive to include in the model but play an important role in determining the azimuthal location of the peak wind. Future versions of the model will attempt to include enhancements that take into account asymmetric wind field mechanisms.

### 7.7. Marine surface layer

Once the mean PBL motion field is determined, the surface wind is estimated through surface layer modeling. Monin-Obukov heights provide an estimate of the importance of shear- or mechanically produced turbulence to buoyancy-produced turbulence. The large values of Monin-Obukov heights computed in tropical cyclones by Moss and Rosenthal [28] and Powell [29] are consistent with shear-induced turbulence associated with neutral, well-mixed surface layers. Hence, a neutral stability surface layer is assumed to exist. In these conditions we can specify the surface stress and friction velocity in terms of a drag coefficient, and use the well-known log profile to describe the variation of wind speed with height. The mean boundary layer (MBL) depth is assumed to be 500 m, and the MBL wind speed is assumed to apply to the midpoint of this layer or 250 m. The MBL height assumption is consistent with mean GPS sonde wind speed profiles [26] which depict the maximum winds at 500 m. A log profile for neutral stability is assumed to apply from the surface (10 m) to 250 m. Recent research on marine boundary layer wind profiles in tropical cyclones [26] supports this assumption to at least 150 m. The mean surface wind for marine exposure is assumed to be 80% of the slab boundary layer wind, in accordance with recent results from boundary layer wind profiles measured in tropical cyclones (Ref. [26]):

$$\left|\vec{U}_{10}\right| \approx 0.8|V|. \tag{12}$$

There is considerable variability in the factor used to estimate the mean surface wind speed. The standard deviation of the reduction factor in (12) is about 10% but this is further complicated by profile failures in extreme conditions and the fact that the profiles are representative of open ocean conditions, rather than coastal onshore flow. When sufficient eyewall wind profiles become available near the coast, it is conceivable that a more sophisticated approach would involve sampling from a statistical distribution of coastal marine boundary layer reduction factors. The height of the model surface wind is 10 m in accordance with the American Society for Testing and Materials (ASTM) standard practice for characterizing surface wind [30] and is assumed to represent a mean over a 1 h time period [13]. We should note that the appropriate time period to assign the model wind speed is not well known and could be adjusted based on how well the model compares to observations. Other hurricane risk models assign wind speed averaging time periods of 20–60 min (see Refs. [13,19]), while real-time hurricane wind analyses using surface winds estimated with model-adjusted flight-level or GPS sonde MBL measurements typically assume 5–10 min averaging periods.

Marine roughness is modeled using the Large and Pond [27] drag coefficient (10) to compute friction velocity given the mean surface wind speed, and then solving the neutral stability log law for $Z_0$. The Large and Pond [27] expression for drag coefficient was found to compare well with open-ocean measurements in hurricanes
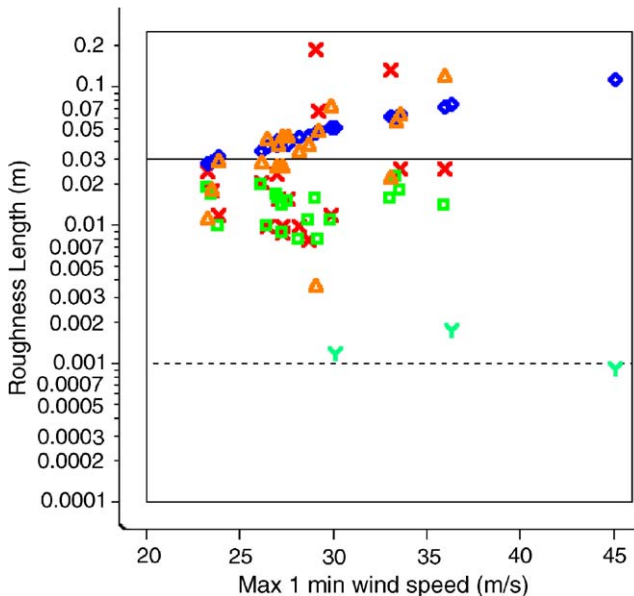


Fig. 7. Dependence of coastal roughness on maximum 1 min sustained wind speed for onshore flow. Preliminary measurements from Cape Hatteras in the eyewall of Hurricane Isabel, courtesy of the State of Florida Coastal Monitoring Program. Isabel measurements [29], from 5 m (squares), 10 m (x), profile method (triangle), Large and Pond's [27] drag coefficient relationship (diamonds), and open ocean [23] measurements from other hurricanes (Y).

for wind speeds up to hurricane force. For higher wind speeds, recent hurricane measurements [26] suggest that the drag coefficient and roughness decrease with wind speed over the open ocean. However, sea state conditions during the landfall of a hurricane are very different from those over the open ocean. Anctil and Donelan [31] suggest that shoaling conditions in the shallow water adjacent to the coastline cause increased roughness and drag coefficient. An extrapolation of the Large and Pond [27] expression to hurricane wind speeds yields $C_d$ values larger than those observed over the open ocean. This behavior is consistent with additional surface layer turbulence associated with coastal wave breaking and shoaling conditions. Further justification for our approach comes from preliminary results of coastal roughness measurements within 200 m of the shore recently obtained during the landfall of Hurricane Isabel at Cape Hatteras by the State of Florida Coastal Monitoring Program [32]. These unique measurements (Fig. 7) in onshore flow document roughness values measured by the turbulent intensity method at 5 and 10 m heights, in addition to the profile method. Although there is considerable scatter among the different methods, the results are consistent with the Large and Pond [27] estimates and more than an order of magnitude larger than open-ocean roughness [26] in similar wind speeds. Further measurements are needed to see if this behavior persists for winds greater than a Saffir–Simpson category one hurricane, and for onshore flow without possible effects of intervening dunes.

## 8. Land friction influences

To standardize observations for a common terrain [33], the mean surface wind for marine conditions is converted to "open terrain" conditions over land using the expression given in Simiu and Scanlan [34]. Improved techniques for converting between large and small roughness regimes are the subject of a future model enhancement. For each 10 min segment of storm motion, the open terrain exposure surface wind speed and direction is determined for all population-weighted zip code centroid locations within the damage threshold distance from the storm center. The open terrain wind at each zip code centroid is corrected to the observed terrain using a fetch-dependent effective roughness for that particular direction and zip code. The effective roughness takes into account the flow over upstream flow obstacles and assumes that internal boundary layer development prevents the flow from reaching complete equilibrium with its surroundings [33,35]. The flow is most influenced by the roughness of the terrain 3 km upstream of the zip code centroid, but the flow is still influenced by terrain further upstream. The approach we use is based on the Source Area Model (SAM) described in Schmidt and Oke [36] and implemented by Axe [37]. SAM takes into account turbulence created by patchy terrain and determines the relative importance of the turbulence source area on a downstream wind sensor located at the zip code centroid. This approach is an improvement over current models that consider zip code roughness constant for all wind directions. Our method is especially advantageous for coastal zip code locations since flow with an upstream fetch over the sea can be significantly stronger than flow over a constant
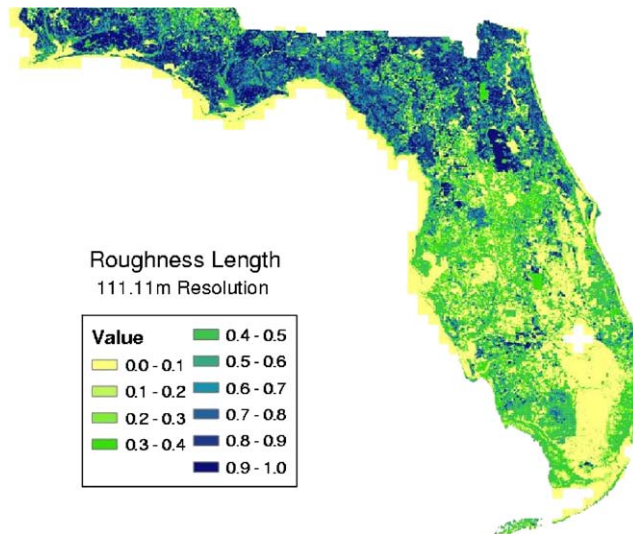
Fig. 8. Distribution of aerodynamic roughness (m) for the State of Florida determined from multi-resolution land-use land-cover classifications.

land roughness. The geographic distribution of roughness (Fig. 8) is associated with a classification of the land use/land cover (LU/LC) in a particular region according to high resolution (50 m) LANDSAT imagery used to develop the National Multi-Resolution Land Cover database [38]. Determination of the roughness for each LU/LC classification was developed by the National Institute for Building Sciences for FEMA's multi hazard damage mitigation model (HAZUS). A limitation of the LU/LC method is that only 21 classifications are available with only two corresponding to developed residential areas. Florida Water Management District LU/LC databases include additional classifications but only three residential classifications. Detailed analysis of airborne lidar data is expected to provide more accurate distributions of surface roughness in the future.

A gust factor [33,39] is used to convert the mean surface wind for the appropriate fetch-dependent roughness to a maximum sustained one min wind as required by the State of Florida Commission on Hurricane Loss Projection, and to a peak 3 s gust as required for the engineering component damage calculations. The same effective roughness is used for the mean wind and gusts. We should caution that the equilibrium fetch lengths for gusts and mean winds are not the same and a more sophisticated fetch modeling approach may be needed to address this in the future. An example of the model wind field for three 2004 hurricanes affecting Florida Hurricane are shown in Fig. 9. At the end of a simulation, time series of wind speed and direction exist for all zip codes in Florida for which hurricanes (or hurricanes that have decayed to a weaker status) have passed within the damage threshold distance. An advantage of our approach over other models is that the complete time series of the wind may be retained at high resolution. Retaining this information makes possible the determination of additional damage-relevant parameters such as
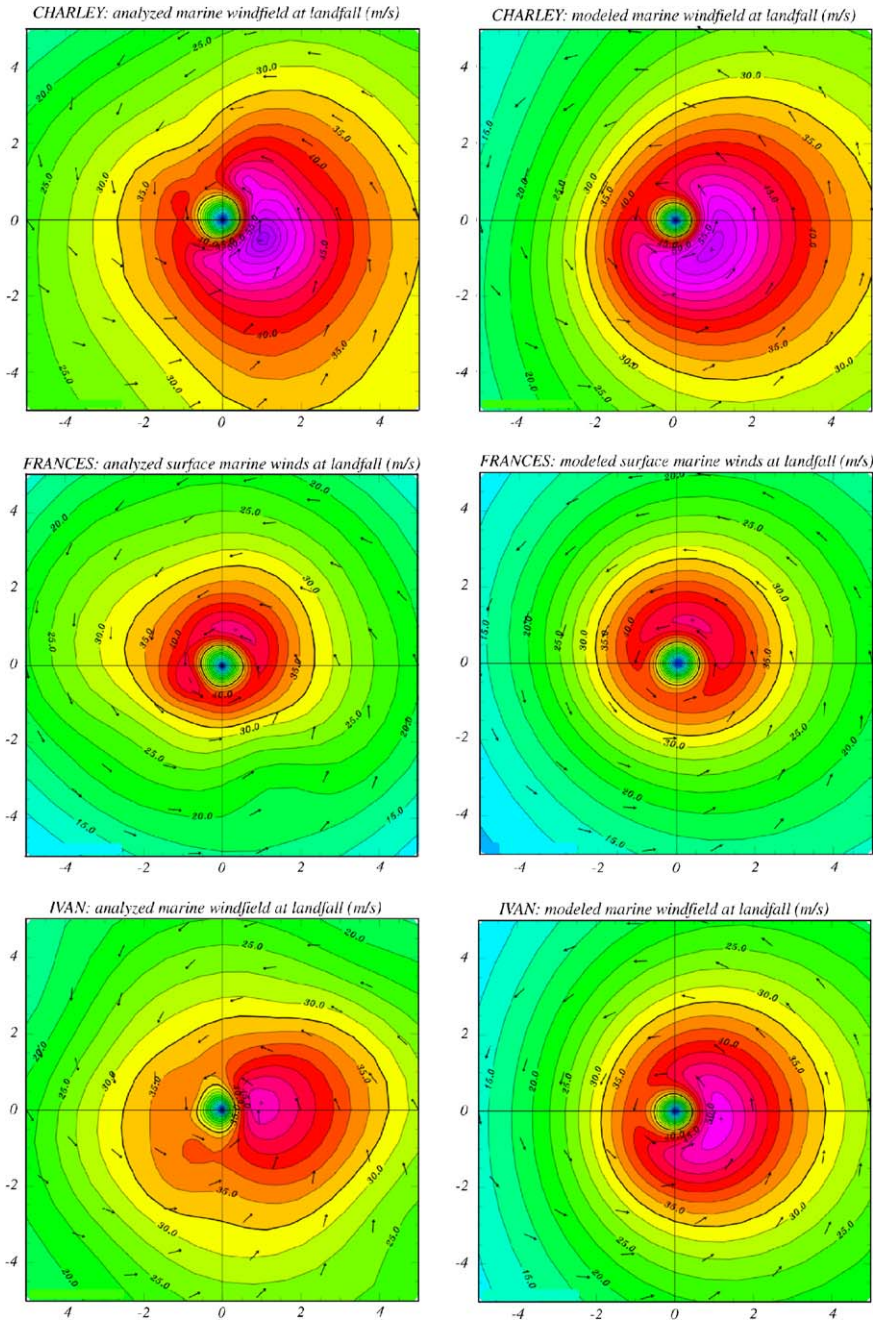
Fig. 9. Comparisons of model surface wind field to observation based H*Wind analyses of 2004 Hurricanes Charley, Frances, and Ivan. Wind fields represent maximum sustained (1 min) surface wind speeds (m/s) for marine exposure. Scaled horizontal coordinate is $R/R_{max}$, North is at top of figure.

duration of winds exceeding hurricane force and wind steadiness. Powell et al. [40] showed that the highest damage observed in Hurricane Andrew was associated with large values of duration and small values of wind direction steadiness. These parameters capture the physical torques of thousands of gust-lull cycles acting on a structure. In addition, given the susceptibility of residential buildings to damage at roof corners and gables, the more the wind direction changes during a strong wind event, the greater the chance that a given wind direction will occur for which a structure is susceptible. Currently the time series capability is available only for scenario simulations. A future enhancement of the model will relate the duration and wind direction unsteadiness to the vulnerability functions contained in the engineering damage component of the model.

## 9. Validation and certification

The track and intensity model will be validated by comparison to historical distributions of landfalls by intensity, translation speed, and Saffir–Simpson category along the Florida coastline. The wind model accuracy will be validated by statistics of grid point comparisons of model fields to observation-based wind field analyses (Fig. 9) as well as to wind speed and direction time series measurements at selected locations. The model is scheduled for submission in 2005 to the State of Florida Commission on Hurricane Wind Loss Projection [41]. The submission process involves satisfying a rigorous set of published standards and providing required disclosures. Independent review of all model components are necessary before submission. A second review is completed on-site by a team of professionals who report to the Commission. Finally the Commission will formally review the model. A positive result will certify the model for use in Florida.

## 10. Conclusions

A Monte Carlo simulation model has been constructed to estimate average annual loss from hurricane wind damage to residential properties. The model is open in the sense that all results will be accessible to the public and the methodology will be completely documented and available for examination. The model incorporates results of many recent research advances while keeping it basic enough to run in a reasonable amount of time. In order to reduce sampling error, a very large simulation ($\sim$50,000–100,000 years of activity) is prescribed. It is expected that the model would be run once per year to take advantage of the latest historical data to assess annual wind exceedance probabilities at each zip code in Florida. Such information can then be provided to the engineering and actuarial components of the model to assess average annual loss for any given residential property exposure portfolio. At present, the wind model calculation requires minutes of computation time per storm, requiring the simulations to be distributed among a number of powerful workstations. The primary user will be the Florida Department of

Financial Services, insurance companies, and homeowners in the state of Florida. There are also many research uses for the model and it is expected that annual enhancements will be required to keep up with the state of the art. The model will reside at Florida International University's International Hurricane Research Center in Miami. Complete documentation of the model algorithms and code will be available for public examination. Given that there may be one Florida hurricane landfall per simulation year, a large number of storms will be contained in our database. Each storm may effect as many as 50 zip codes so it is expected that the database could contain several million records for track, intensity, and landfall wind field information on each storm. The database could then be queried for details on simulated storms and wind exceedance probability distributions relevant to a given zip code or county in Florida.

## Appendix A. Hurricane model equations and integration

### A.1. Definitions

| | |
|---|---|
| $r_{max}$ | radius of maximum surface wind speed, specified |
| $c_t$ | storm translation speed, specified from storm track |
| $c_{dir}$ | storm translation direction compass heading, specified from storm track |
| $\Delta_p$ | central pressure deficit, specified |
| $p(r) = p_0 + \Delta p e^{-(r_{max}/r)^B}$ | sea level pressure |
| $B$ | Holland profile parameter |
| $\phi$ | Azimuthal coordinate, measured counterclockwise from east |
| $s = r/R_{max}$ | normalized radial coordinate |
| $v_g(s)$ | Gradient wind: $v_g^2/s + r_{max} f v_g = (1/\rho)(\partial p/\partial s)$ |
| $f = 2\Omega \sin\Theta$ | Coriolis parameter |
| $\Theta$ | latitude of storm center |

| | |
|---|---|
| $\Omega$ | earth angular acceleration |
| $v_0(s)$ | normalized gradient wind (symmetric) $= v_g(s)/v_{gmax}$, where $v_{gmax}$ is the maximum gradient wind in the radial profile |
| $\bar{f} = r_{max}f/v_{g\,max}$ | normalized Coriolis parameter |
| $v(s, \phi) = v/v_{g\,max}$ | normalized storm-relative tangential wind component |
| $u(s, \phi) = u/v_{g\,max}$ | normalized storm-relative radial wind component |
| $\alpha$ | friction coefficient, $r_{max}C_d/h$ |
| $h$ | mean boundary layer height |
| $C_d$ | drag coefficient |
| $c = c_t/v_{g\,max}$ | normalized translation speed |

$$g(s) = 2v_0(s)s^{-1} + \bar{f}, \tag{A.1}$$

$$d(s) = \dot{v}_0 + v_0 s^{-1} + \bar{f}, \tag{A.2}$$

where a "dot" represents a derivative with respect to $s$, $g(s)$ and $d(s)$ depend only on $v_0$ and $\bar{f}\sigma(s, \phi) = v(s, \phi) - v_0(s)$ normalized departure from gradient balance.

### A.2. Scaling of the governing equations prior to implementation

Substituting the terms from the above definitions and changing the radial coordinate from $r$ to $s$, the steady-state form of the governing equations (4) and (5) become:

$$u\partial_s u + s^{-1}(v_0 + \sigma)\partial_\phi u - \sigma(g + s^{-1}\sigma) + \alpha(u + c\,\sin\,\phi)(w - c) = 0, \tag{A.3}$$

$$u\partial_s \sigma + s^{-1}(v_0 + \sigma)\partial_\phi \sigma + u(d + s^{-1}\sigma) + \alpha(v_0 + \sigma + c\,\cos\,\phi)(w - c) = 0, \tag{A.4}$$

$$w = \sqrt{(u + c\,\sin\,\phi)^2 + (v_0 + \sigma + c\,\cos\,\phi)^2}, \tag{A.5}$$

where $w$ is the total normalized earth-relative wind.

In the event that $c$ vanishes, so that the cyclone is stationary, these equations reduce to the ordinary differential equations:

$$u\dot{u} - \sigma(g + s^{-1}\sigma) + \alpha uw = 0, \tag{A.6}$$

$$u(\dot{\sigma} + s^{-1}\sigma + d) + \sigma(v_0 + \sigma)w = 0, \tag{A.7}$$

$$w = \sqrt{u^2 + (v_0 + \sigma)^2} \tag{A.8}$$

for the radial profiles $u(s)$ and $\sigma(s)$. Here, "." indicates differentiation with respect to $s$.

*A.3. Wind model implementation*

Eqs. (A.3) and (A.4) supplemented by (A.5), constitute two, coupled, time independent partial differential equations for the storm relative radial velocity $u$ and the storm relative departure from gradient balance $s$. The storm relative tangential wind is then given by $v = v_g + s$. Unfortunately, the direct numerical solution of (A.3) and (A.4) is time consuming even though the equations are time-independent because the non-linear coupling of the terms necessitates an iterative numerical approach.

However, Eqs. (A.6) and (A.7), can readily be numerically integrated to furnish a completely symmetric wind field fully described by the radial profiles $u(s)$ and $v(s) = v_g(s) + \sigma(s)$.

The functions $u(s)$ and $s(s)$ so obtained can serve as radial profiles for the construction of basis functions for a more realistic attack on (A.3) and (A.4).

Namely, we put forth the ansatz:

$$u(s, \phi) = \mathrm{ff}u(\phi)u(s), \tag{A.9}$$

$$\sigma(s, \phi) = \mathrm{ff}\sigma(\phi)\sigma(s), \tag{A.10}$$

where the azimuthal dependence is introduced through the form factors:

$$\mathrm{ff}u(\phi) = a_0 + a_1 \cos \phi + a_2 \sin \phi, \tag{A.11}$$

$$\mathrm{ff}\sigma(\phi) = b_0 + b_1 \cos \phi + b_2 \sin \phi. \tag{A.12}$$

Now the six coefficients $a_0$, $a_1$, $a_2$ and $b_0$, $b_1$, $b_2$ can be variationally determined by substituting (A.9) and (A.10) into the left-hand sides of (A.3) and (A.4), supplemented by (A.5) to form the "residuals" RA3 and RA4. We then form the functional

$$J(a, b) = \frac{\sum |\mathrm{RA3}| + |\mathrm{RA4}|}{\mathrm{NGRID}}, \tag{A.13}$$

where the sum is taken over every spatial point for which the profiles and trigonometric functions are known (polar grid) and NGRID is the total number of such grid points.

$J$ then depends solely on the unknown coefficients $a_0$, $a_1$, $a_2$ and $b_0$, $b_1$, $b_2$. These coefficients are chosen to minimize $J$ and so furnish us with an approximate solution for $u,(s,\phi)$ and $\sigma(s,\phi)$, from which we form the storm relative radial and tangential wind components $u_r$ and $v_t$, namely:

$$u_r(s, \phi) = u(s, \phi) \text{ and } v_t(s, \phi) = v_g(s, \phi) + \sigma(s, \phi), \tag{A.14}$$

By adding the translational velocity $c$ (in polar coordinates) to $u_r$ and $v_t$ we obtain the earth-relative components of the windfield $u_{er}$ and $v_{er}$:

$$u_{er}(s, \phi) = u_r(s, \phi) + c \sin \phi, \tag{A.15}$$

$$v_{er}(s, \phi) = v_r(s, \phi) + c \cos \phi, \tag{A.16}$$

where $c$ is the normalized translation speed $c = c_t/v_{gmax}$.

Finally, since (A.3), (A.4) and (A.5) refer to a cyclone moving along the *Y*-axis, the entire generated wind field grid must be rotated so that the *Y*-axis of the calculation coincides with the actual compass direction of motion of the translating cyclone.

## References

[1] C.J. Neumann, B.R. Jarvinen, C.J. McAdie, G.R. Hammer, Tropical Cyclones of the North Atlantic Ocean, 1871–1998, National Oceanic and Atmospheric Administration, 1999, 206pp.

[2] L.R. Russell, Probability distributions for hurricane effects, J. Waterways Harbors Coastal Eng. Div. ASCE 97 (1971) 139–154.

[3] M.E. Batts, M.R. Cordes, L.R. Russell, E. Simiu, Hurricane wind speeds in the United States, National Bureau of Standards, Report no BSS-124, US Department of Commerce, 1980.

[4] C.W. Landsea, R.A. Pielke Jr., A.M. Mestas-Nunez, J.A. Knaff, Atlantic basin hurricanes: indices of climatic changes, Climatic Change 42 (1999) 89–129.

[5] B.R. Jarvinen, C.J. Neumann, M.A.S. Davis, A tropical cyclone data tape for the North Atlantic basin 1886–1963: contents limitations and uses, NOAA Technical Memo NWS NHC 22, National Hurricane Center, 1984, 22pp.

[6] R.W.R. Darling, Estimating probabilities of hurricane wind speeds using a large scale empirical model, J Climate 4 (1991) 1035–1046.

[7] R. Rotunno, K.A. Emanuel, An air-sea interaction theory for tropical cyclones, Part II. Part I, J. Atmos. Sci. 42 (1987) 1062–1071.

[8] H.E. Willoughby, M.D. Shoreibah, Concentric eyewalls, secondary wind maxima, and the evolution of the hurricane vortex, J. Atmos. Sci. 39 (1982) 395–411.

[9] M.D. Powell, S.H. Houston, Hurricane Andrew's landfall in South Florida. Part II: surface wind fields and potential real-time applications, Weather Forecast. 11 (1996) 329–349.

[10] L.K. Shay, G.J. Goni, P.G. Black, Effects of a warm oceanic feature on Hurricane Opal, Mon. Weather Rev. 125 (5) (2000) 1366–1383.

[11] B.I. Miller, A study on the filling of Hurricane Donna (1960) over land, Mon. Weather Rev. 92 (1964) 389–406.

[12] M.D. Powell, The transition of the Hurricane Frederic boundary layer wind field from the open Gulf of Mexico to landfall, Mon. Weather Rev. 110 (1982) 1912–1932.

[13] P.J. Vickery, L.A. Twisdale, Wind field and filling models for hurricane wind speed predictions, . Struct. Eng. 121 (1995) 1700–1709.

[14] F.P. Ho, J.C. Su, K.L. Hanevich, R.J. Smith, F.P. Richards, Hurricane climatology for the Atlantic and Gulf coasts of the United States, NOAA Technical Memo NWS 38, NWS Silver Spring, MD, 1987.

[15] R.E. Tuleya, M.A. Bender, Y. Kurihara, A simulation study of the landfall of tropical cyclones using a movable nested-mesh model, Mon. Weather Rev. 112 (1984) 124–136.

[16] J. Kaplan, M. DeMaria, A simple empirical model for predicting the decay of tropical cyclone winds after landfall, J. Appl Meteorol 34 (1995).

[17] K.V. Ooyama, Numerical simulation of the life cycle of tropical cyclones, J. Atmos. Sci. 26 (1969) 3–40.

[18] L. Shapiro, The asymmetric boundary layer flow under a translating hurricane, J. Atmos. Sci. 40 (1983) 1984–1998.

[19] E.F. Thompson, V.J. Cardone, Practical modeling of hurricane surface wind fields, J. Waterways Port Coastal Ocean Eng. Div. ASCE 122 (1996) 195–205.

[20] P.J. Vickery, P.F. Skerjl, A.C. Steckley, L.A. Twisdale, A hurricane wind field model for use in simulations, J. Struct. Eng. 126 (2000) 1203–1222.

[21] P.J. Vickery, P.F. Skerjl, L.A. Twisdale, Simulation of hurricane risk in the United States using an empirical storm track modeling technique, J. Struct. Eng. 126 (2000) 1222–1237.

[22] Y.M. Kurihara, M.A. Bender, R.E. Tuleya, R.J. Ross, Improvements in the GFDL hurricane prediction system, Mon. Weather Rev. 123 (1995) 2791–2801.

[23] G.J. Holland, An analytic model of the wind and pressure profiles in hurricanes, Mon. Weather Rev. 108 (1980) 1212–1218.

[24] H.E. Willoughby, M.E. Rahn, Parametric representation of the primary hurricane vortex Part I: observations and evaluation of the Holland (1980) model, Mon. Weather Rev. 132 (2004) 3033–3048.

[25] M. Demaria, J. Pennington, K. Williams, Description of the Extended Best track file (EBTRK1.4) version 1.4, Available from NESDIS/CIRA/Regional and Mesoscale Meteorology Team, Colorado State University, Fort Collins, CO, 2002.

[26] M.D. Powell, P.J. Vickery, T. Reinhold, Reduced drag coefficient for high wind speeds in tropical cyclones, Nature 422 (2003) 279–283.

[27] W.G. Large, S. Pond, Open ocean momentum flux measurements in moderate to strong winds, J. Phys. Oceanogr. 11 (1981) 324–336.

[28] M.S. Moss, S.L. Rosenthal, On the estimation of planetary boundary layer variables in mature hurricanes, Mon. Weather Rev. 106 (1975) 841–849.

[29] M.D. Powell, Evaluations of diagnostic marine boundary layer models applied to hurricanes, Mon.Weather Rev. 108 (1980) 757–766.

[30] ASTM, Standard practice for characterizing surface wind using a wind vane and rotating anemometer, D 5741-96, Annual Book of ASTM Standards, vol. 11.03, 1996.

[31] F. Anctil, M. Donelan, Air–water momentum flux observations over shoaling waves, J. Phys. Oceanogr. 26 (1996) 1344–1353.

[32] T. Reinhold, K. Gurley, Florida Coastal Monitoring Program, 2003; http://www.ce.ufl.edu/~fcmp.

[33] M.D. Powell, S.H. Houston, T. Reinhold, Hurricane Andrew's landfall in south Florida. Part I: standardizing measurements for documentation of surface wind fields, Weather Forecast. 11 (1996) 304–328.

[34] E. Simiu, R.H. Scanlan, Wind Effects on Structures: Fundamentals and Applications to Design, Wiley, New York, 1996.

[35] E.W. Peterson, Modification of mean flow and turbulent energy by a change in surface roughness under conditions of neutral stability, Q.J.R. Meteorol. Soc. 95 (1969) 561–575.

[36] H.P. Schmidt, T.R. Oke, A model to estimate the source area contributing to turbulent exchange in the surface layer over patchy terrain, Q.J.R. Meteorol. Soc. 116 (1990) 965–988.

[37] L.M. Axe, Hurricane surface wind model for risk assessment, M.S. Thesis, Department of Meteorology, Florida State University, 2003.

[38] J.E. Vogelmann, S.M. Howard, L. Yang, C.R. Larson, B.K. Wylie, N. Van Driel, Completion of the 1990s National land cover data set for the conterminous United States from landsat thematic mapper data and ancillary data sources, Photogramm. Eng. Remote Sens. 67 (2001) 650–652.

[39] P.J. Vickery, P.F. Skerlj, Hurricane gust factors revisited, J. Struct. Eng. 131 (2005) 825–832.

[40] M.D. Powell, S.H. Houston, I. Ares, Real-time damage assessment in hurricanes, The 21st AMS Conference on Hurricanes and Tropical Meteorology, Miami, FL, April 24–28, 1995, Paper 12A.4 pp. 500–502.

[41] Commission 2004, Report of Activities as of November 1, 2004, Florida Commission on Hurricane Loss Projection Methodology, available from www.fsba.state.fl.us/methodology/meetings.asp